

Quantum Criticality of Valence Transition for the Unique Electronic State of Antiferromagnetic Compound EuCu_2Ge_2

Jun Gouchi^{1*}, Kazumasa Miyake², Wataru Iha³, Masato Hedo⁴, Takao Nakama⁴, Yoshichika Ōnuki⁴, and Yoshiya Uwatoko¹

¹*Institute for Solid State Physics, University of Tokyo, Kashiwa, Chiba 277-8581, Japan*

²*Center for Advanced High Magnetic Field Science, Graduate School of Science, Osaka University, Toyonaka, Osaka 560-0043, Japan*

³*Graduate School of Engineering and Science, University of the Ryukyus, Nishihara, Okinawa 903-0213, Japan*

⁴*Faculty of Science, University of the Ryukyus, Nishihara, Okinawa 903-0213, Japan*

The effect of pressure on the unique electronic state of the antiferromagnetic (AF) compound EuCu_2Ge_2 has been measured in a wide temperature range from 10 mK to 300 K by electrical resistivity measurements up to 10 GPa. The Néel temperature of $T_N = 15$ K at ambient pressure increases monotonically with increasing pressure and becomes a maximum of $T_N = 27$ K at 6.2 GPa but suddenly drops to zero at $P_c \simeq 6.5$ GPa, suggesting the quantum critical point (QCP) of the valence transition of Eu from a nearly divalent state to that with trivalent weight. The $\rho_{\text{mag}0}$ and A values obtained from the low-temperature electrical resistivity based on the Fermi liquid relation of $\rho_{\text{mag}} = \rho_{\text{mag}0} + AT^2$ exhibit huge and sharp peaks around P_c . The exponent n obtained from the power law dependence $\rho_{\text{mag}} = \rho_{\text{mag}0} + BT^n$ is clearly less than 1.5 at $P = P_c \simeq 6.5$ GPa, which is expected at the AF-QCP. These results indicate that P_c coincides with P_v , corresponding to the quantum criticality of the valence transition pressure P_v . The electronic specific heat coefficient γ , estimated from the generalized Kadowaki-Woods relation, is about 510 mJ/(mol·K²) around P_c , suggesting the formation of a heavy-fermion state.

Most Eu compounds including $\text{Eu}_2\text{Ni}_3\text{Ge}_5$ ¹⁾ and EuRhSi_3 ¹⁾ order magnetically because of the divalent electronic state of Eu^{2+} . Valence instability often occurs in Eu compounds, from the divalent electronic state of $\text{Eu}^{2+}(4f^7: S = 7/2, L = 0, \text{ and } J = 7/2)$ at high temperatures to the nearly nonmagnetic electronic state ($4f^6$ in $\text{Eu}^{3+}: S = L = 3, \text{ and } J = 0$) at low tem-

*gouchi@issp.u-tokyo.ac.jp

peratures, upon changing the magnetic field and pressure. Here, S , L , and J denote the spin, orbital, and total angular momenta, respectively. These compounds can be used to construct a conventional pressure phase diagram.¹⁾ That is very similar to the Doniach phase diagram for the Ce compounds.²⁻⁴⁾ According to the result of the electrical resistivity measurement of $\text{Eu}_2\text{Ni}_3\text{Ge}_5$, which is an antiferromagnet with $T_N = 19$ K and exhibits a successive change of the antiferromagnetic (AF) structure at $T'_N = 17$ K, the Eu valence transition is not realized but the Eu valence changes continuously as a function of pressure.¹⁾ The Néel temperature T_N increases with applying pressure up to 6 GPa, starts to decrease with further increasing pressure, and most likely becomes zero at around $P_c = 12\text{-}13$ GPa. A similar trend is also realized in EuRhSi_3 .¹⁾

In the case of EuRh_2Si_2 , on the other hand, the Eu valence is nearly divalent and EuRh_2Si_2 orders antiferromagnetically in the low-temperature region. The Néel temperature of $T_N = 23.8$ K increases as a function of pressure. The change in valence, which is realized in the pressure region of $0.96 \text{ GPa} < P < 2 \text{ GPa}$, is surprisingly very sharp, indicating the first-order phase transition from nearly divalent to nearly trivalent.^{5,6)} With further increasing pressure, its electronic state approaches the trivalent state. EuCo_2Ge_2 exhibits a similar trend.⁷⁾

Recently, chemical- and high-pressure measurements have been carried out on single crystals of $\text{EuCu}_2(\text{Si}_x\text{Ge}_{1-x})_2$ grown by the Bridgman method.⁸⁾ EuCu_2Ge_2 with the ThCr_2Si_2 -type tetragonal structure undergoes two successive transitions at $T_N \sim 15$ K and $T'_N \sim 9$ K, while EuCu_2Si_2 shows no magnetic orderings at ambient pressure. T_N slightly increases with increasing x and starts decreasing at $x = 0.5$, and T_N disappears around $x \simeq 0.7$, revealing a mixed-valence or valence-fluctuating state. Similar behavior is observed in Ce-based heavy-fermion compounds.²⁻⁴⁾ In the case of EuCu_2Si_2 ($x = 1$), on the other hand, an intermediate valence state was indicated by resistivity, specific heat, and magnetic susceptibility measurements. EuCu_2Si_2 is not in the Eu-divalent state but is close to the Eu-trivalent state. These results are consistent with those of previous studies on a series of $\text{EuCu}_2(\text{Si}_x\text{Ge}_{1-x})_2$.⁹⁾ Replacing Ge by Si leads to a chemical compression and indicates the transition from the nearly trivalent state ($x < 0.65$) to a heavy-fermion state ($0.65 < x < 0.85$) and then to a nonmagnetic state.

In the case of EuCu_2Ge_2 , the effective magnetic moment μ_{eff} , obtained from the inverse magnetic susceptibility⁸⁾ and Mössbauer spectroscopy,¹⁰⁾ is close to the free-ion value $\mu_{\text{eff}} = 7.94\mu_B/\text{Eu}$ of Eu^{2+} . $T_N = 15$ K at ambient pressure increases as a function of pressure, becomes a maximum of $T_N = 27$ K at 6 GPa, and decreases steeply toward zero at a pressure between $P = 6$ and 7 GPa. Both the A and ρ_0 values, obtained by assuming the low-temperature

resistivity $\rho = \rho_0 + AT^2$ based on the Fermi liquid relation, exhibit pronounced peaks at around $P = 7$ GPa. The determined value of A is approximately $0.23 \mu\Omega \text{ cm K}^{-2}$ at 7 GPa. It corresponds to $370 \text{ mJ / (mol} \cdot \text{K}^2)$ if we assume the relation of the generalized Kadowaki-Woods plot ($N = 4$), namely, $A/\gamma^2 = 2 \times 10^{-5}/N(N-1) \simeq 0.17 \times 10^{-5} \mu\Omega \text{ cm (K mol/mJ)}^2$, where N is the degeneracy of f -levels.¹¹⁾ These results suggest that the effective mass of EuCu_2Ge_2 is highly enhanced at around 7 GPa. From X-ray absorption experiments,¹²⁾ the valence continuously changes from 1 to 6 GPa. In the higher-pressure region, the strong magnetic interaction is replaced by the pure valence fluctuations and the valence of Eu increases up rapidly up to 20 GPa. The advantage of a pressure experiment is that it maintains the sample as clean as possible, in contrast to alloying as $\text{EuCu}_2(\text{Si}_x\text{Ge}_{1-x})_2$. The abrupt drop of T_N in a very narrow pressure region is highly different from the two cases mentioned above, which are described by the Doniach picture as in $\text{Eu}_2\text{Ni}_3\text{Ge}_5$ ¹⁾ and the valence transition as in EuRh_2Si_2 .^{5,6)} This suggests that there is a new physical mechanism that cannot be understood within the conventional point of view of the phase change under pressure. However, the pressure ranges in the measurement described in Ref. 8 are not narrow enough considering the sharp disappearance of T_N , indicating the need to perform measurements with finer intervals of pressure up to 10 GPa and down to much lower temperatures 10 mK. In this paper, we report the results of such resistivity measurements that reveal a new aspect of the transition at $P = P_c$, where the AF order disappears discontinuously.

Single crystals of EuCu_2Ge_2 were grown by the Bridgman method using a Mo crucible, as described detail in a previous paper.⁸⁾ The electrical resistivity was measured by a conventional ac four-probe method using a Linear Research LR-700 ac resistance bridge. The current flow J was chosen to be parallel to the tetragonal [100] direction. High pressure experiments were performed by using a palm cubic anvil cell, which is known to generate hydrostatic pressure owing to the multiple-anvil geometry.¹³⁾ A mixture of Flourinert 70 and 77 were used as a pressure medium. The pressure was determined using a laboratory-built calibration table, which was calibrated by detecting the characteristic phase transitions of Bi, Sn, and Pb.¹³⁾ The pressure cell was set to a dilution refrigerator using BlueFors LD-400 and cooled to 10 mK.

Figures 1(a) and 1(b) show the temperature dependences of the electrical resistivity ρ under several pressures, together with the data for YCu_2Si_2 ¹⁴⁾ as a reference of the phonon parts of EuCu_2Ge_2 . At ambient pressure, the electrical resistivity decreases almost linearly with decreasing temperature and becomes constant below 30 K. The step like increase and decrease in resistivity correspond to the AF transition at $T_N = 15$ K and $T'_N = 8.9$ K, respec-

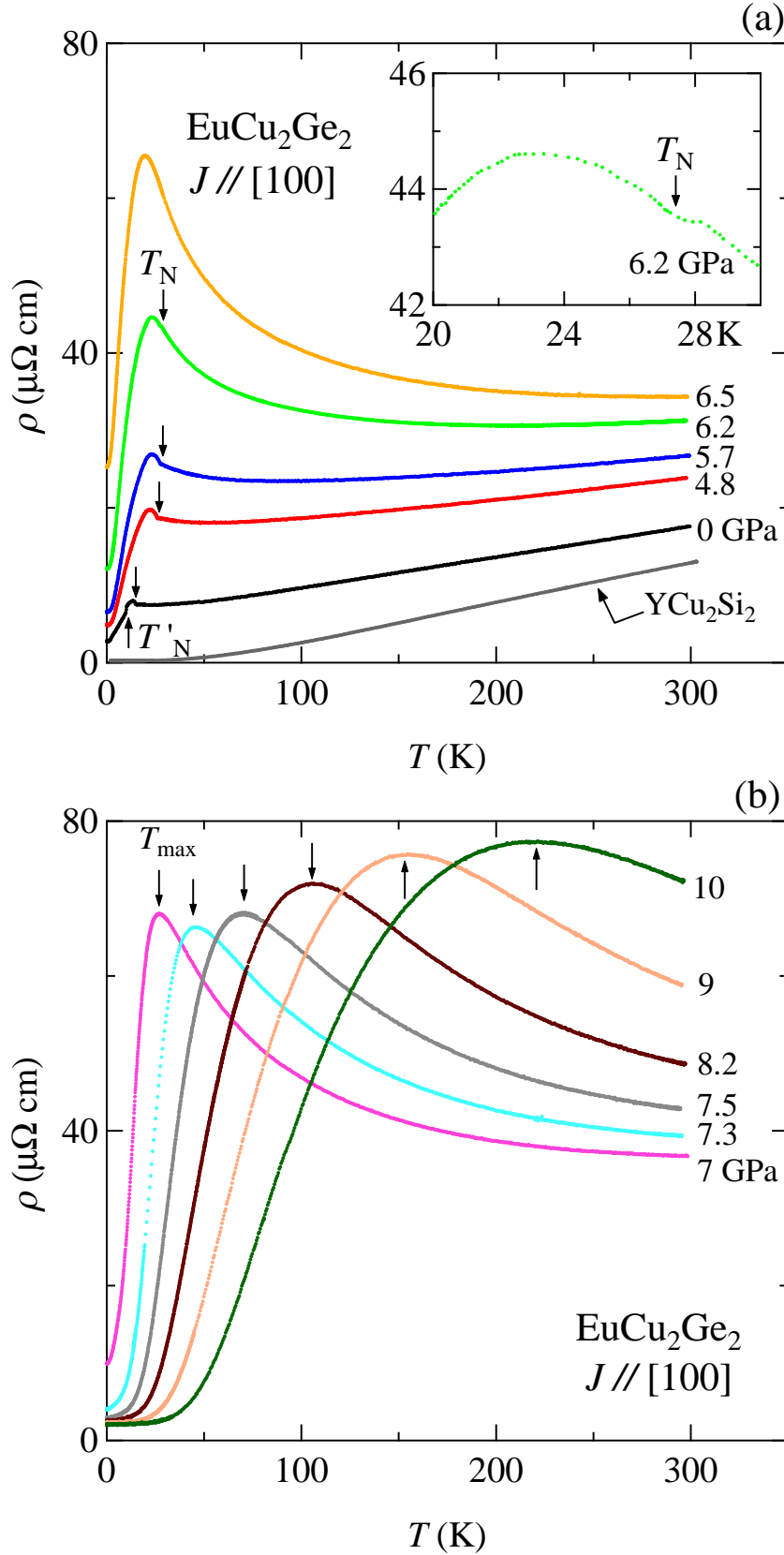


Fig. 1. (color online) Temperature dependences of the electrical resistivity in EuCu_2Ge_2 (a) up to 6.5 GPa and (b) up to 10 GPa. The arrows indicate (a) the AF transitions and (b) T_{max} . The inset of (a) shows a magnified view of the electrical resistivity at 6.2 GPa.

tively. With increasing pressure, the resistivity at room temperature increases because the c - f hybridization between conduction electrons and $4f$ electrons is enhanced. T_N substantially increases from 15 K and becomes maximum at about 27 K at 6.2 GPa. Although T_N at 6.2 GPa is unclear in a wide temperature region, a slight change can be found as shown in the inset of Fig. 1(a). The temperature dependences of ρ in EuCu_2Ge_2 are similar to the resistivity results for $\text{Eu}_2\text{Ni}_3\text{Ge}_5$ ¹⁾ and $\text{EuCu}_2(\text{Si}_x\text{Ge}_{1-x})_2$.⁸⁾ They suggest that the valence of Eu increases continuously from nearly divalent to trivalent with increasing pressure. There is no anomaly reflecting the valence transition T_v at low temperatures. These data are similar to the recently reported ones and the temperature dependences of ρ under high pressures are reminiscent of the Kondo effect in Ce-based heavy-fermion compounds.²⁻⁴⁾ The resistivity at 6.5 GPa indicates no clear magnetic ordering and is typical for a moderate heavy-fermion state. Note that T'_N disappears rapidly under pressure, where it was not observed at 2 GPa in a previous experiment.⁸⁾ The temperature dependence of the electrical resistivity at 6.5 GPa resembles that of $\text{EuCu}_2(\text{Si}_x\text{Ge}_{1-x})_2$ with $x = 0.6$, where the Néel temperature decreases rapidly with increasing concentration x . The electrical resistivity possesses a peak around $T_{\text{max}} = 20$ K under pressure and it is characteristic of the Kondo behavior, where T_{max} is defined as the Kondo temperature. The resistivity shows a $-\log T$ dependence. T_{max} remains up to 6.5 GPa and shifts to higher temperatures with further increasing pressure. The qualitative behavior of the electrical resistivity of EuCu_2Ge_2 under higher pressures will gradually approach that of EuIr_2Si_2 ,¹⁵⁾ which is a nonmagnetic compound and exhibits a broad maximum around 200 K in $\rho(T)$.

From these data, we present the pressure P vs Néel temperature T_N phase diagram of EuCu_2Ge_2 in Fig. 2. The Néel temperature T_N becomes a maximum at $P = 6.2$ GPa and drops to zero very sharply at 6.5 GPa. In the previous high-pressure study of $\text{Eu}_2\text{Ni}_3\text{Ge}_5$,¹⁾ the Néel temperature was found to increase to 7 GPa but to decrease continuously with further increasing pressure, suggesting that the valence changed continuously as a function of pressure. The Kondo-like behavior of the electrical resistivity of EuCu_2Ge_2 at $T > T_{\text{max}}$ suggests the existence of a heavy-fermion state at low temperatures above P_c . In the present study, on the other hand, the Néel temperature became zero abruptly at around 6.5 GPa. This suggests that the valence of Eu increased continuously up to $P = 6.2$ GPa, and then the quantum critical point (QCP) of the valence transition or sharp crossover of the valence arises abruptly at around $P = 6.5$ GPa.

The theoretical understanding of Ce and Yb compounds has already been discussed in Refs. 16 and 17. Indeed, this phenomenon of EuCu_2Ge_2 resembles a pressure effect on the

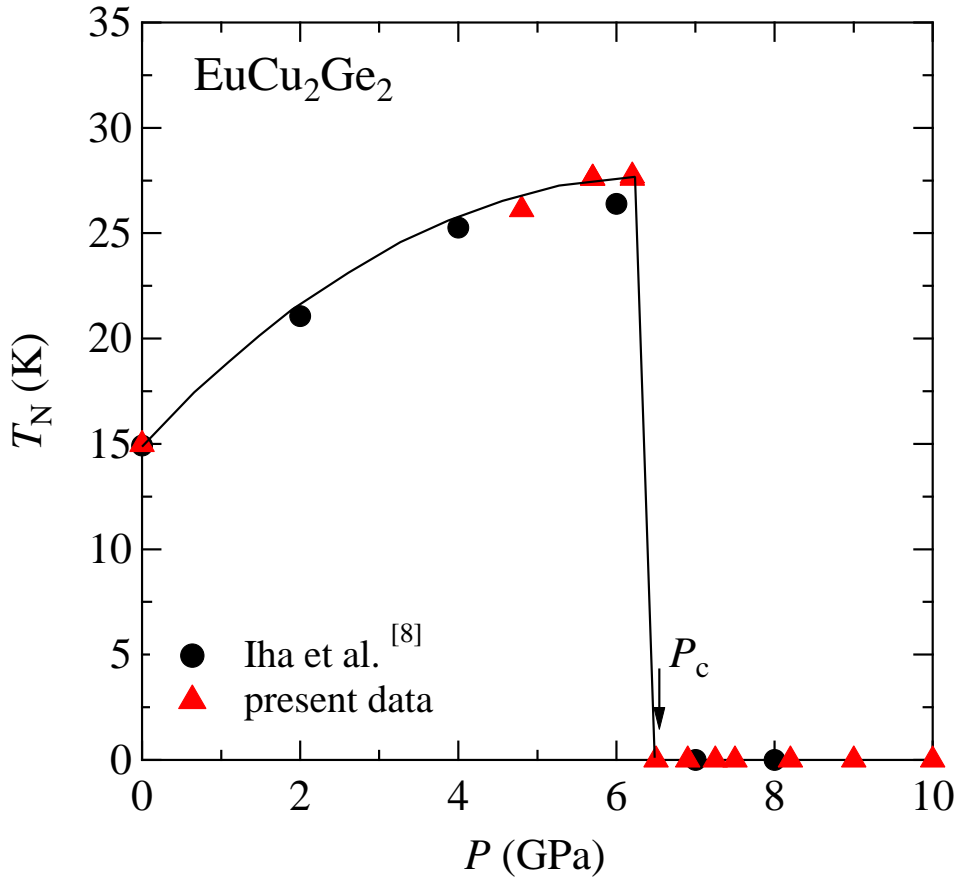


Fig. 2. (color online) Pressure-Néel temperature phase diagram in EuCu_2Ge_2 .

prototypical heavy-fermion compound CeRhIn_5 in which the AF order disappears suddenly at $P = P_c \approx 2.4$ GPa under a magnetic field of $H > 4$ T,^{18,19)} which is associated with the Fermi surface change from a small to a large one as observed in a de Haas-van Alphen experiment.²⁰⁾ These behaviors have been understood theoretically in a unified fashion as a phenomenon that the sharp crossover or the criticality of the valence change cuts the AF order discontinuously in the case where the strength of the c - f hybridization is relatively small.^{16,21)}

We consider here the Fermi liquid relation $\rho_{\text{mag}} = \rho_{\text{mag}0} + AT^2$ where the antiferromagnetic ordering disappeared. The magnetic resistivity ρ_{mag} is estimated by subtracting the electrical resistivity of YCu_2Si_2 (phonon part)¹⁴⁾ from that of EuCu_2Ge_2 as $\rho_{\text{mag}} = \rho(\text{EuCu}_2\text{Ge}_2) - \rho(\text{YCu}_2\text{Si}_2)$ in order to remove the phonon contribution. $\rho_{\text{mag}0}$ was determined by the magnetic residual resistivity at the lowest temperature of measurement, i.e., 10 mK. Figure 3 shows the pressure dependences of $\rho_{\text{mag}0}$ and the coefficient A assuming that the Fermi liquid relation of $\rho_{\text{mag}} = \rho_{\text{mag}0} + AT^2$ holds in the paramagnetic state. The Fermi liquid relation that

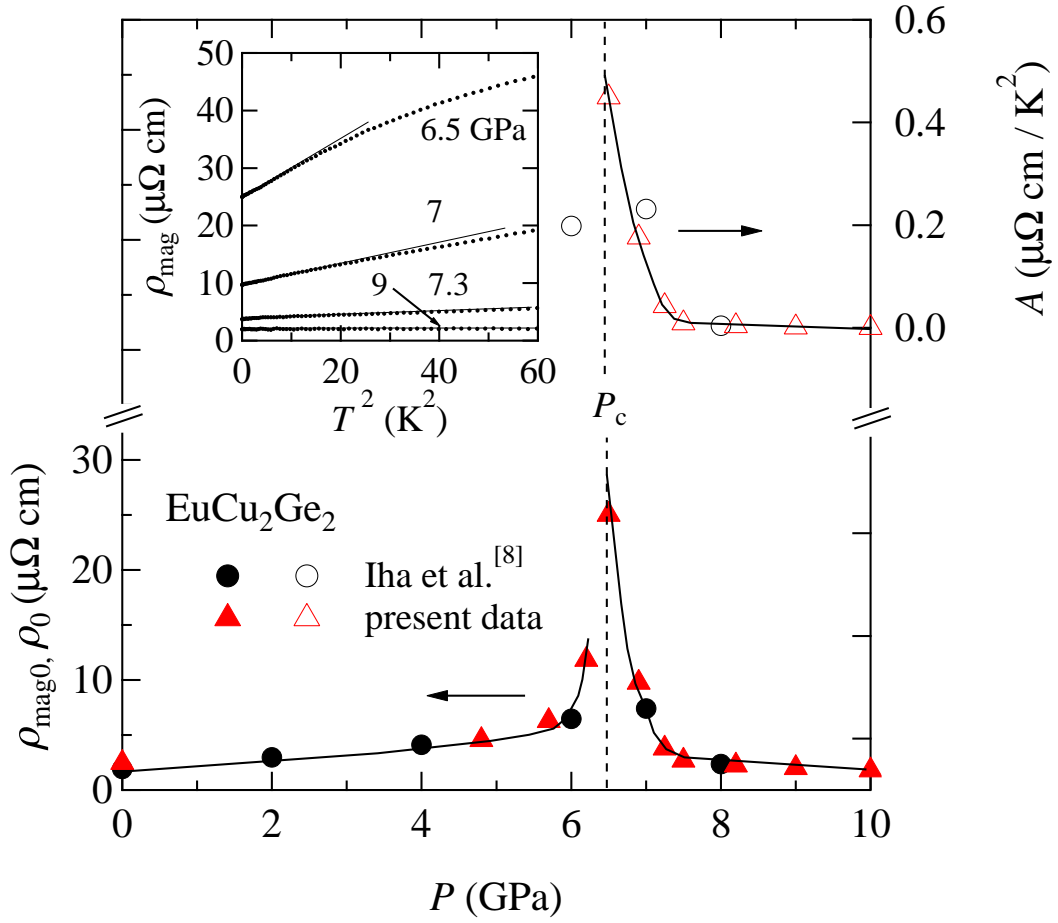


Fig. 3. (color online) Pressure dependences of the coefficient of the T^2 dependence of the electrical resistivity A , residual resistivity ρ_0 , and magnetic residual resistivity $\rho_{\text{mag}0}$. The solid lines serve as a visual guide. The circular and triangular symbols indicate our previous and present data, respectively. The open and closed symbols indicate the coefficient A and ρ_0 or $\rho_{\text{mag}0}$, respectively. Note that the closed circles and triangles indicate residual resistivity ρ_0 and $\rho_{\text{mag}0}$, respectively. The inset shows the T^2 dependence of ρ_{mag} at low temperatures.

persists up to about 1.8 K at 6.5 GPa spreads to a higher-temperature range as pressure is increased, as shown in the inset of Fig. 3. Correspondingly, $\rho_{\text{mag}0}$ increases moderately as a function of pressure up to $P = 6$ GPa. However, $\rho_{\text{mag}0}$ increases steeply toward the sharp and huge peak at $P = P_c \simeq 6.5$ GPa, as shown in the lower part of Fig. 3. This supports the fact that this critical pressure P_c is related with the QCP of the valence transition as discussed in Ref. 22. The values of A were obtained assuming the Fermi liquid relation. The obtained A , which is proportional to the enhanced effective electron mass, decreases substantially above P_c . The present A value is $0.45 \mu\Omega \text{ cm K}^{-2}$ at 6.5 GPa and corresponds to $510 \text{ mJ/mol}\cdot\text{K}^2$ if we assume the generalized Kadowaki-Woods relation as mentioned above. This implies that the

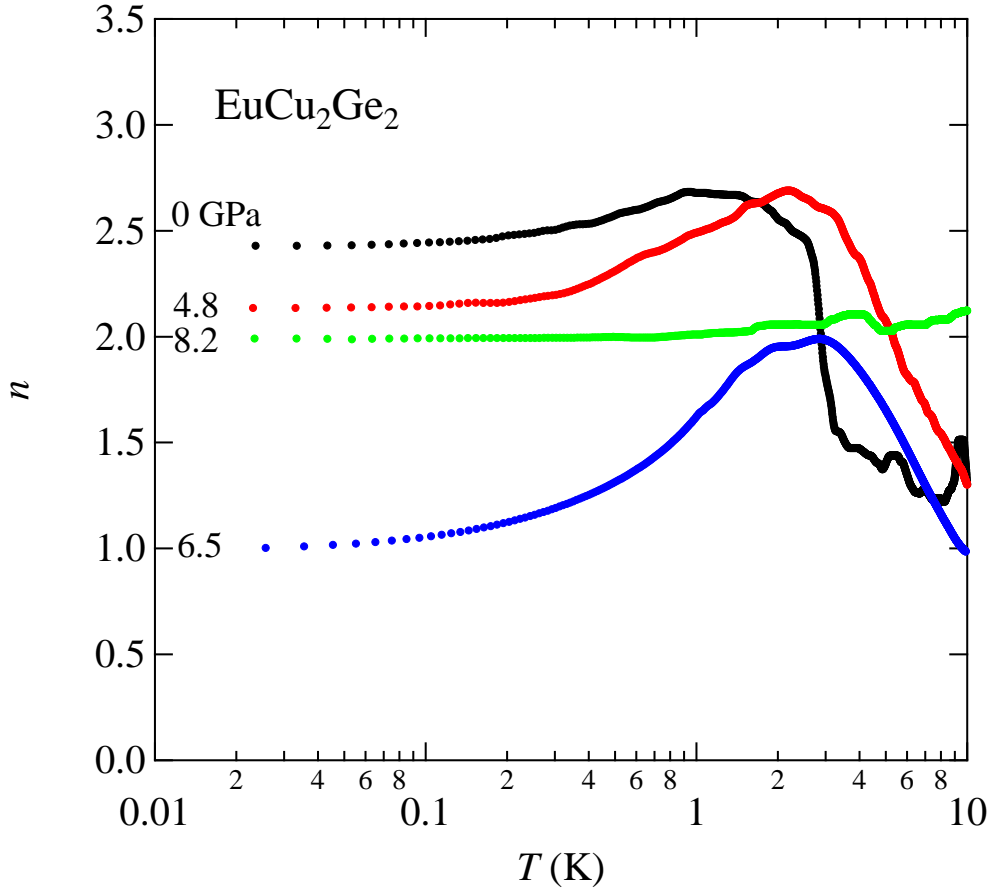


Fig. 4. (Color online) Power-law behavior for selected resistivity curves on a semilog scale.

effective mass of quasiparticles is highly enhanced according to the generalized Kadowaki-Woods relation^{23,24)} or the temperature dependence of $\rho(T)$ changes from T^2 to T^n with a smaller exponent of $n < 2$ due to the quantum criticality in one form or another.

Next, we focus on the pressure effect on the exponent n of the power law dependence of the resistivity: $\rho_{\text{mag}} = \rho_{\text{mag}0} + BT^n$. The fit of the power law $\rho_{\text{mag}} = \rho_{\text{mag}0} + BT^n$ to the resistivity data provides valuable information on the pressure dependences of the exponent n of EuCu_2Ge_2 . It is predicted that n reaches 1.5 for the AF-QCP,²⁵⁾ while it reaches 1 for the QCP of the valence transition.²⁶⁾ In the present study, AF ordering abruptly disappears at 6.5 GPa, which is consistent with the change in the valence of Eu from nearly divalent toward the trivalent state. Indeed, there is evidence for the quantum valence fluctuations as discussed below.

Figure 4 shows the temperature dependence of the power-law behavior for selected resis-

tivity curves, where the exponent n is defined as

$$n \equiv \frac{\partial \log(\rho_{\text{mag}} - \rho_{\text{mag}0})}{\partial \log T}. \quad (1)$$

In this analysis, $\rho_{\text{mag}0}$ was used for the same value as shown in Fig. 3. Figure 5 shows the pressure dependence of exponent n . In the magnetic region ($0 < P < 6.2$ GPa), n is larger than the Fermi liquid value $n = 2$, probably due to electron-magnon scattering. Approaching P_c , the exponent n decreases as a function of pressure and approaches $n = 1$ slightly above 6.5 GPa, suggesting that P_c coincides with P_v , the critical pressure for the quantum valence transition. Because n is markedly changed, even with a slight change in pressure, the tuning of pressure around P_c is very difficult in experiments. Since the exponent n appreciably deviates from 1.5 at $P = 6.5$ GPa, the scenario based on critical AF fluctuations²⁵⁾ cannot be applied to the present case but suggests that P_c ($= P_v$) is located at slightly higher than $P = 6.5$ GPa, which is consistent with the huge peak of $\rho_{\text{mag}0}$ at $P = 6.5$ GPa as discussed in Refs. 22 and 27. Namely, the scenario based on critical valence fluctuations explains a gross feature of pressure effect on n and $\rho_{\text{mag}0}$ of EuCu_2Ge_2 observed near the critical pressure $P_c \simeq 6.5$ GPa. Similar behavior was observed also in CeCu_2Ge_2 ²⁸⁾ and CeRhIn_5 .¹⁸⁾ In the case of CeCu_2Ge_2 ,²⁸⁾ the exponent n decreases rapidly with increasing pressure in the antiferromagnetic region and crosses almost exactly the value of $n = 1$ at $P = P_c$, and the P -interval where n is smaller than two corresponds approximately to that of superconductivity. Also, in the case of CeRhIn_5 , the exponent of n approaches $n = 1$ near $P = P_c$.^{18,19)} This is a signature of critical valence fluctuations. In the present pressure experiment, we did not observe superconductivity in EuCu_2Ge_2 , unlike the cases of CeCu_2Ge_2 and CeCu_2Si_2 in which the superconducting transition temperature is enhanced at around P_v .^{27,28)}

In summary, we have studied the pressure effect on the electronic state of the AF compound EuCu_2Ge_2 . The Néel temperature substantially increases from 15 K as a function of pressure and becomes a maximum of $T_N = 27$ K at 6.2 GPa. The resistivity at 6.5 GPa indicates no clear magnetic transition. In the present system, the valence of Eu changed continuously with increasing pressure up to 6.2 GPa, following the Doniach phase diagram. At $P_c \simeq 6.5$ GPa, the Néel temperature abruptly dropped to zero, suggesting that a sharp or critical valence change occurs there from nearly a divalent state to one with a trivalent component of Eu^{3+} . The exponent n obtained from the power law $\rho_{\text{mag}} = \rho_{\text{mag}0} + BT^n$ is very close to $n = 1$ at $P = 6.5$ GPa. These results indicate that the case occurs where the pressure just above $P = 6.5$ GPa coincides with P_v , corresponding to the quantum criticality of the valence transition. This is the first observation of this phenomenon among

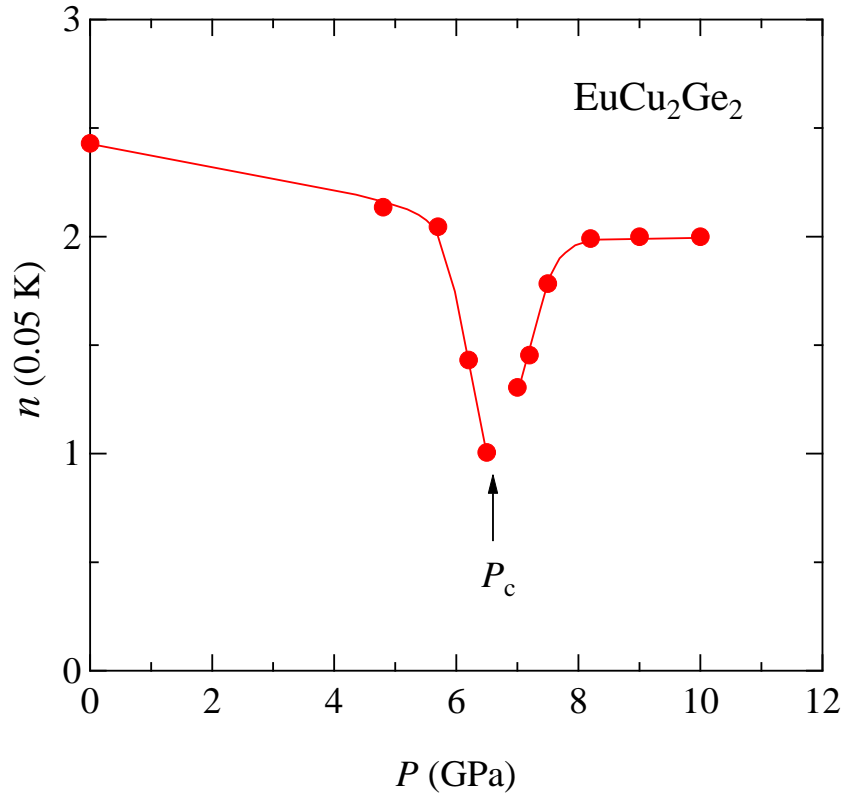


Fig. 5. (Color online) Pressure dependence of exponent n of the power law $\rho_{\text{mag}} = \rho_{\text{mag}0} + BT^n$ of the magnetic resistivity at 0.05 K for EuCu_2Ge_2 . The solid curves are guides to the eye.

the Eu compounds. The electronic specific heat coefficient, estimated from the generalized Kadowaki-Woods plot, was about $510 \text{ mJ/mol}\cdot\text{K}^2$, suggesting that the effective mass of the quasiparticles is highly enhanced around P_c .

Acknowledgements

We thank S. Nagasaki for helping with our high-pressure experiments. This work was partially supported by JSPS KAKENHI Grant Numbers JP19H00648, JP18H04329, JP17K05547, JP17K05555, and JP16K05453.

References

- 1) M. Nakashima, Y. Amako, K. Matsubayashi, Y. Uwatoko, M. Nada, K. Sugiyama, M. Hagiwara, Y. Haga, T. Takeuchi, A. Nakamura, H. Akamine, K. Tomonori, T. Yara, Y. Ashitomi, M. Hedō, T. Nakama, and Y. Ōnuki, *J. Phys. Soc. Jpn.* **86**, 034708 (2017).
- 2) N. D. Mathur, F. M. Grosche, S. R. Julian, I. R. Walker, D. M. Freye, R. K. W. Haselwimmer, and G. G. Lonzarich, *Nature* **394**, 39 (1998).
- 3) R. Movshovich, T. Graf, D. Mandrus, J. D. Thompson, J. L. Smith, and Z. Fisk, *Phys. Rev. B* **53**, 8241 (1996).
- 4) G. R. Stewart, *Rev. Mod. Phys.* **73**, 797 (2001).
- 5) A. Mitsuda, S. Hamano, N. Araoka, H. Yamaya, and H. Wada, *J. Phys. Soc. Jpn.* **81**, 023709 (2012).
- 6) F. Honda, K. Okauchi, A. Nakamura, D. Li, D. Aoki, H. Akamine, Y. Ashitomi, M. Hedō, T. Nakama, and Y. Ōnuki, *J. Phys. Soc. Jpn.* **85**, 063701 (2016).
- 7) Y. Ashitomi, M. Kakihana, F. Honda, A. Nakamura, D. Aoki, Y. Uwatoko, M. Nakashima, T. Takeuchi, T. Kida, T. Tahara, M. Hagiwara, Y. Haga, M. Hedō, T. Nakama, and Y. Ōnuki, *Physica B* **536**, 192 (2018).
- 8) W. Iha, T. Yara, Y. Ashitomi, M. Kakihara, T. Takeuchi, F. Honda, A. Nakamura, D. Aoki, J. Gouchi, Y. Uwatoko, T. Kida, T. Tahara, M. Hagiwara, Y. Haga, M. Hedō, T. Nakama, and Y. Ōnuki, *J. Phys. Soc. Jpn.* **87**, 064706 (2018).
- 9) S. Fukuda, Y. Nakanuma, J. Sakurai, A. Mitsuda, Y. Ishikawa, F. Ishikawa, T. Goto, and T. Yamamoto, *J. Phys. Soc. Jpn.* **72**, 3189 (2003).
- 10) P. Wang, Z. M. Stadnik, J. Żukrowski, B. K. Cho, and J. U. Kim, *Solid State Commun.* **150**, 2168 (2010).
- 11) N. Tsujii, H. Kontani, and K. Yoshimura, *Phys. Rev. Lett.* **94**, 057201 (2005).
- 12) A. Y. Geondzhian, A. A. Yaroslavl'tsev, P. A. Alekseev, R. V. Chernikov, B. R. Gaynanov, F. Baudelet, L. Nataf, and A. P. Menushenkov, *J. Phys.: Conf. Ser.* **712**, 012112 (2016).
- 13) J. -G. Cheng, K. Matsubayashi, S. Nagasaki, A. Hisada, T. Hirayama, M. Hedō, H. Kagi, and Y. Uwatoko, *Rev. Sci. Instrum.* **85**, 093907 (2014).
- 14) N. D. Dung, T. D. Matsuda, S. Ikeda, E. Yamamoto, Y. Haga, Y. Takeda, T. Endo, Y. Doi, R. Settai, H. Harima, and Y. Ōnuki, *J. Phys. Soc. Jpn.* **77**, 094702 (2008).
- 15) Y. Ōnuki, A. Nakamura, D. Aoki, M. Boukahil, Y. Haga, T. Takeuchi, H. Harima, M. Hedō, and T. Nakama, *J. Phys.: Conf. Series* **592**, 012049 (2015).

- 16) S. Watanabe and K. Miyake, J. Phys.: Condens. Matter **23**, 094217 (2011).
- 17) K. Miyake and S. Watanabe, J. Phys. Soc. Jpn. **83**, 061006 (2014).
- 18) G. Knebel, D. Aoki, J.-P. Brison, and J. Fouquet, J. Phys. Soc. Jpn. **77**, 114704 (2008).
- 19) T. Park, V. A. Sidorov, F. Ronning, J.-X. Zhu, Y. Tokiwa, H. Lee, E. D. Bauer, R. Movshovich, J. L. Sarrao, and J. D. Thompson, Nature **456**, 366 (2008).
- 20) H. Shishido, R. Settai, H. Harima, and Y. Ōnuki, J. Phys. Soc. Jpn. **74**, 1103 (2005).
- 21) S. Watanabe and K. Miyake, J. Phys. Soc. Jpn. **79**, 033707 (2010).
- 22) K. Miyake and H. Maebashi, J. Phys. Soc. Jpn. **71** 1007 (2002).
- 23) K. Kadowaki and S. B. Woods, Solid State Commun. **58**, 507 (1986).
- 24) K. Miyake, T. Matsuura, and C. M. Varma, Solid State Commun. **71**, 1149 (1989).
- 25) T. Moriya and T. Takimoto, J. Phys. Soc. Jpn. **64**, 960 (1995).
- 26) A. T. Holmes, D. Jaccard, and K. Miyake, Phys. Rev. B **69**, 024508 (2004).
- 27) D. Jaccard, H. Wilhelm, K. Alami-Yadri, and E. Vargoz, Physica B **259-261**, 1 (1999).
- 28) H. Wilhelm, K. Alami-Tadri, B. Revaz, and D. Jaccard, Phys. Rev. B **59**, 3651 (1999).